6th European Conference on Computational Mechanics (ECCM 6)
7th European Conference on Computational Fluid Dynamics (ECFD 7)
11-15 June 2018, Glasgow, UK

CROUZEIX-RAVIART MULTISCALE FINITE ELEMENT METHOD FOR STOKES FLOWS IN HETEROGENEOUS MEDIA

Q.FENG[1], G.ALLAIRE[2] and M.A.PUSCAS[3]

[1,3] CEA-Saclay
Gif-sur-Yvette, 91191 cedex, France
{qingqing.feng, maria-adela.puscas}@cea.fr

[2] CMAP/Ecole Polytechnique
route de Saclay, 91128 Palaiseau Cedex, France
gregoire.allaire@polytechnique.fr and http://www.cmap.polytechnique.fr/∼allaire/

Key words: Multiscale Finite Element Method, Crouzeix- Raviart Element, Stokes Flow, Heterogeneous Media.

Abstract. This paper addresses a non-conforming Multiscale Finite Element Method (MsFEM) for viscous incompressible flows in genuine heterogeneous media. The multiscale method relies upon the coupling of two grid scales: one coarse grid and one fine grid. The principe is to compute on the fine grid effective properties of the media in the form of basis functions, which are then used to solve problems on the coarse grid [1]. It's known that when computing multiscale basis functions, the approximation of boundary conditions on coarse element edges influences critically the accuracy of the MsFEM. Based on the work of [2], the weakly enforced conformity between coarse elements leads to a natural boundary condition on coarse element edges. This relaxes the sensitivity of the method to complex patterns of obstacles, without any need of oversampling techniques. Two methods have been developped and compared making use of a study of open flows in a heterogeneous domain.

1 INTRODUCTION

Many engineering problems have multi-scale features, composite materials and flows in porous medai are typical examples of such kind. In some cases, the quantities of interest are only related to the large-scale properties of the solutions, but the fine-scale features of the model can have significant impact on the large-scale properties of the solutions. However, one needs a very fine mesh to resolve the fine-scale features of the problem to get faithful numerical results. Thus many Multiscale Finite Element method (MsFEM) are developed to solve multiscale problems without being confined to solving fine scale solutions. A nuclear reactor core can be considered as a porous media due to the existence of thousands of fuel rods. In order to efficiently solve this highly heterogeneous problem, a Multiscale Finite Element Method (MsFEM) is thus desired.

Firstly talked in the work of [3], when computing multiscale basis functions, the approximation of boundary conditions can influence greatly the eventual accuracy of the MsFEM method. Thus Hou and Wu have introduced the oversampling method to provide a best approximation of the boundary condition of the multiscale basis functions. The method consists of solving local problems in a domain larger than the coarse element itself. The aim is to reduce the effect of wrong boundary conditions and bad sampling sizes.

The non-conforming nature of Crouzeix-Raviart element [4] is shown to provide a good flexibility especially when arbitary patterns of porosities or inclusions are considered. Based on this feature, [2], [5], [6] and [7] have proposed a non-conforming Crouzeix-Raviart MsFEM, where the conformity between coarse elements are enforced on in a weak sense, i.e., only the "jump" of the basis functions vanish at coarse element edges. This leads to a natural boundary condition on coarse element edges, which relaxes the sensitivity of the method to complex patterns of obstacles, without having to use oversampling methods.

Based on [2] and [7], we have implemented Crouzeix-Raviart MsFEM in TrioCFD [8] to solve the Stokes flow in heterogeneous media. We have extended the MsFEM for unstructured meshes and developed techniques in Salome plateform to generate such specific discretizations. No penalization techniques are employed in our computations. Local cell problems are solved by the Finite Volume Element Method (FVEM) instead of the Finite Element Method (FEM). One method to enrich the basis functions is developed in order to improve the accuracy. The paper is organized as follows. The formulation of problem is given in section 2. The construction of Crouzeix-Raviart MsFEM is presented

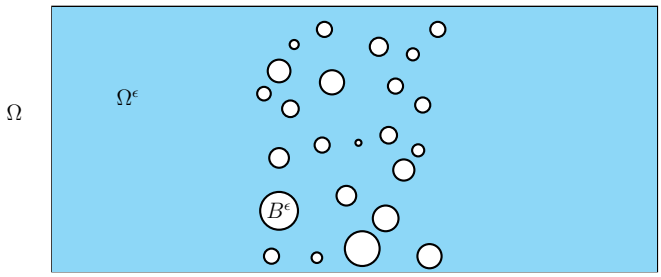

Figure 1: An illustration of domain Ω comprising a fluid domain Ω^ϵ perforated by inclusions B^ϵ

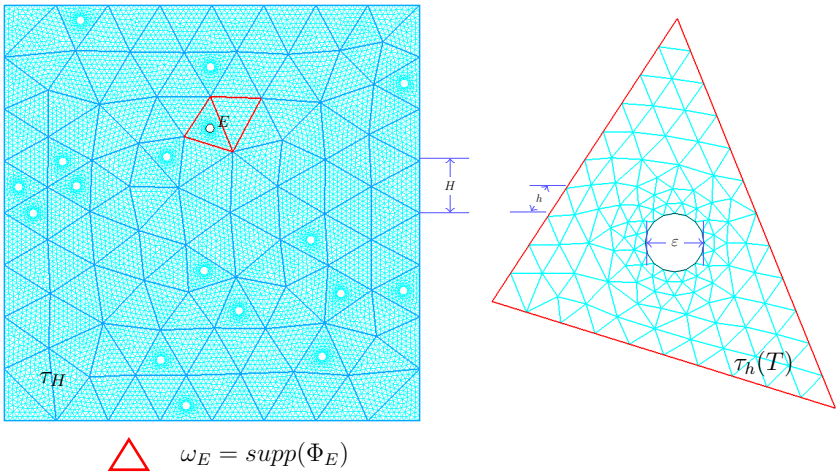

Figure 2: An illustration of the discretised domain τ_H and the ω_E support of $\mathbf{\Phi}_E$.

in section 3. In section 4, numerical tests are presented and results are discussed followed by some conclusions.

2 PROBLEM FORMULATION

We define a domain Ω, a two-dimensional domain consisting of a set of inclusions B^ϵ and the flow domain Ω^ϵ avec $\Omega = \Omega^\epsilon \cup B^\epsilon$ (see Fig. 1). The steady-state Stokes's problem is to find the velocity $\boldsymbol{u}$ and the pressure p which are solutions to:

$$\begin{aligned} -\nu\Delta\boldsymbol{u} + \nabla p &= \boldsymbol{f} \quad \text{in } \Omega^\epsilon \\ \nabla \cdot \boldsymbol{u} &= 0 \quad \text{in } \Omega^\epsilon \end{aligned} \tag{1}$$

The boundary conditions are given by:

$$\begin{aligned} \boldsymbol{u} &= 0 \quad \text{on } \partial B^\epsilon \cap \partial\Omega^\epsilon \\ \boldsymbol{u} &= \boldsymbol{\omega} \quad \text{on } \partial\Omega \cap \partial\Omega^\epsilon \end{aligned} \tag{2}$$

where $\boldsymbol{f}$ is a source function and $\boldsymbol{\omega}$ is a function fixed at the boundary $\partial\Omega$. Here we consider only the non-slip boundary condition on the boundaries of inclusions: $\boldsymbol{\omega} = \mathbf{0}$.

3 APPLICATION OF CROUEIX-RAVIART MsFEM

Here, we explain the application of our method by first defining the coarse and fine meshes. We then introduce the functional spaces for our multiscale basis functions and describe the constuction of these basis functions within each coarse elements.

3.1 Discretisation

We discretise the domain Ω into a two-dimnesional non-structured mesh τ_H (see Fig. 2). τ_H consists of coarse elements T_k, k=1,2,...,N_H, where N_H is the total number of coarse elements. The $\mathcal{E}_H$ the sef of all coarse element edges E_j, j=1,2,...,N_E in τ_H including edges

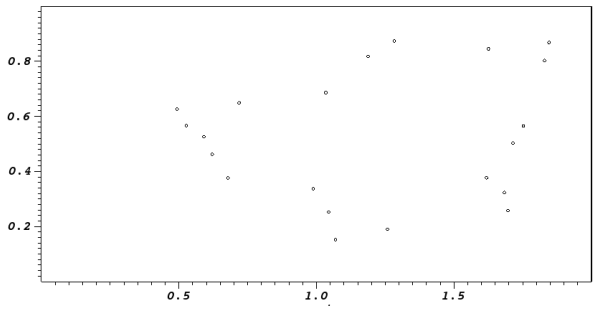

Figure 3: Computational domain with 21 arbitary placed inclusions

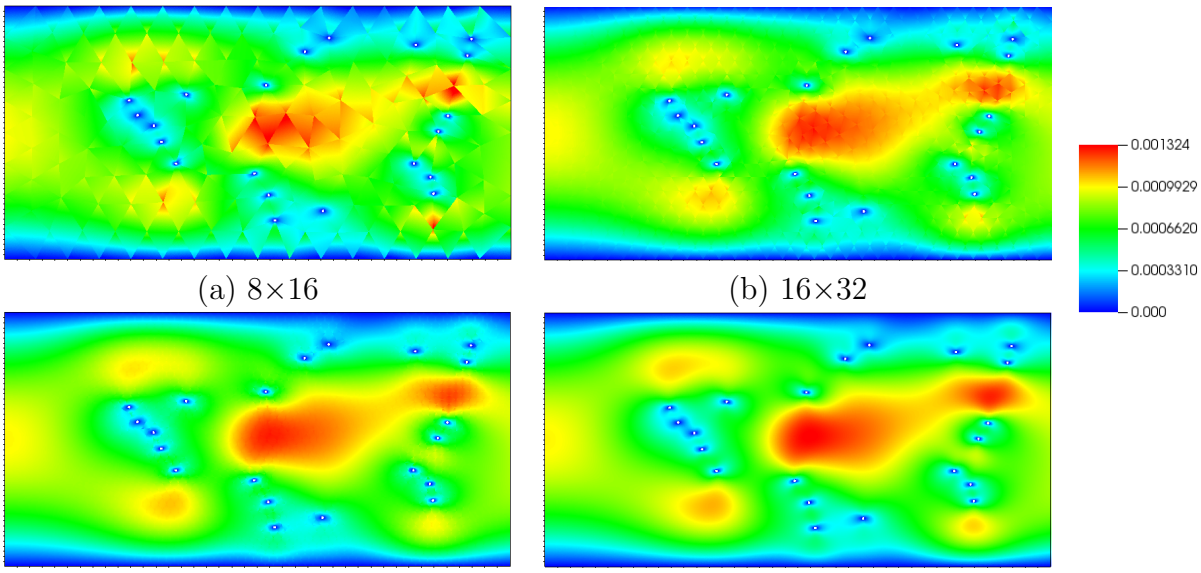

(a) 8×16 (b) 16×32

(c) 32×64 (d) Reference

Figure 4: u_x contours of a channel flow with inclusions with the CR2 method

on the domain boundary $\partial\Omega$. For each coarse element T_k, we construct a fine mesh $\tau_h(T_k)$, consisting of fine elements each with width h. The union of $\tau_h(T_k)$ for all T_k constructs a global fine mesh τ_h, which overlaps with τ_H.

3.2 Crouzeix-Raviart functional spaces

The functional spaces for velcity V_H, and for pressure M_H are given below:

$$
\begin{aligned}
V_H = \{ \quad & \boldsymbol{u} \in \left(L^2(\Omega)\right)^d : \quad \forall T \in \mathcal{T}_H,\ \exists p \in L_0^d\left(\Omega^\epsilon \cap T\right) \text{ such that} \\
& -\Delta \boldsymbol{u} + \nabla p = 0 \qquad \text{on } \Omega^\epsilon \cap T, \\
& \nabla \cdot \boldsymbol{u} = const_1 \qquad \text{on } \Omega^\epsilon \cap T, \\
& \boldsymbol{u} = 0 \qquad \text{on } B^\epsilon \cap T, \\
& \boldsymbol{n} \cdot \nabla \boldsymbol{u} + p\boldsymbol{n} = \boldsymbol{g} \qquad \text{on } E \cap \Omega^\epsilon,\ \forall E \in \mathcal{E}(T) \quad \}
\end{aligned}
\tag{3}
$$

where $\mathcal{E}_H(T)$ is the ensemble of edges composing ∂T and $\boldsymbol{g}$ a linear function. d is the dimension of the domain. The key point is to maintain the continuity of the average of the

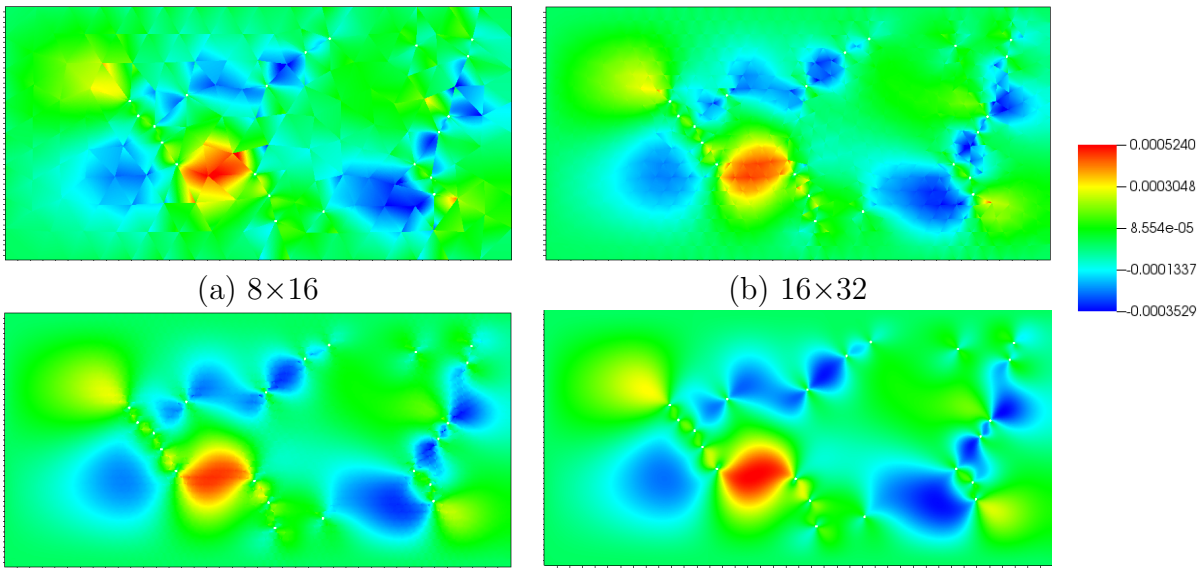

(a) 8×16 (b) 16×32

(c) 32×64 (d) Reference

Figure 5: u_y contours of a channel flow with inclusions with the CR2 method

velocity across an edge E: $\int_E [[u]] \cdot \omega_{E,j} = 0$, where $[[u]] = 0$ is the jump of the velocity across E and $\omega_{E,j}$ are weighting functions associated to the edge E with $j = 1, ..., s$ and s a positive integer. The weak continuity across element boundaries allows adaptive boundary conditions which relaxes the sensitivity of the method to random arrangements of inclusions, without the need of applying any oversampling methods.

3.3 Construction of Crouzeix-Raviart basis

For each edge $E \in \mathcal{E}_H$, we construct the basis functions $\mathbf{\Phi}_{E,i} \in V_H$, such that $\int_E \mathbf{\Phi}_{E,i} = \boldsymbol{e}_i$, and $\int_{E'} \mathbf{\Phi}_{E,i} = 0$ for all $E' \in \mathcal{E}_H$, $E' \neq E$. These basis functions form a basis of V_H, i.e.:

$$V_H = span\{\mathbf{\Phi}_{E,i}, E \in \mathcal{E}_H, i = 1, \cdots, s\}. \tag{4}$$

The support of $\mathbf{\Phi}_{E,i}$ is $supp\,(\mathbf{\Phi}_{E,i}) \subset \omega_E$, which is the ensemble of two adjacent triangles T_k, $k = 1, 2$ in τ_H which share the edge E. We solve on each of these triangles $\mathbf{\Phi}_{E,i}$ and $\pi_{E,i}$:

$$\begin{aligned}
-\Delta \mathbf{\Phi}_{E,i} + \nabla \pi_{E,i} &= 0 \text{ on } \Omega^\epsilon \cap \mathcal{T}_k, \\
\nabla \cdot \mathbf{\Phi}_{E,i} &= const \text{ on } \Omega^\epsilon \cap \mathcal{T}_k, \\
\boldsymbol{n} \cdot \nabla \mathbf{\Phi}_{E,i} - \pi_{E,i} \boldsymbol{n} &\in \text{span}\,\{\boldsymbol{\omega}_{F,1}, \cdots, \boldsymbol{\omega}_{F,s}\} \text{ on } F \cap \Omega^\epsilon \quad \forall F \in \mathcal{E}(\mathcal{T}_k), \\
\mathbf{\Phi}_{E,i} &= 0 \text{ on } B^\epsilon \cap \mathcal{T}_k, \\
\int_F \mathbf{\Phi}_{E,i} \cdot \boldsymbol{\omega}_{F,j} &= \begin{cases} \delta_{ij}, & F = E \\ 0, & F \neq E \end{cases} \quad \forall F \in \mathcal{E}\,(\mathcal{T}_k)\,, j = 1, \cdots, s. \\
\int_{\Omega^\epsilon \cap T_k} \pi_{E,i} &= 0.
\end{aligned} \tag{5}$$

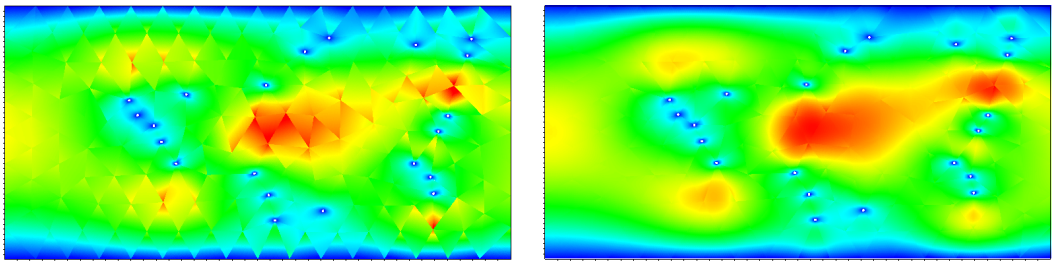

(a) CR2 8×16 (b) CR3 8×16

Figure 6: Comparison of u_x contours computed with CR2 and CR3 methods

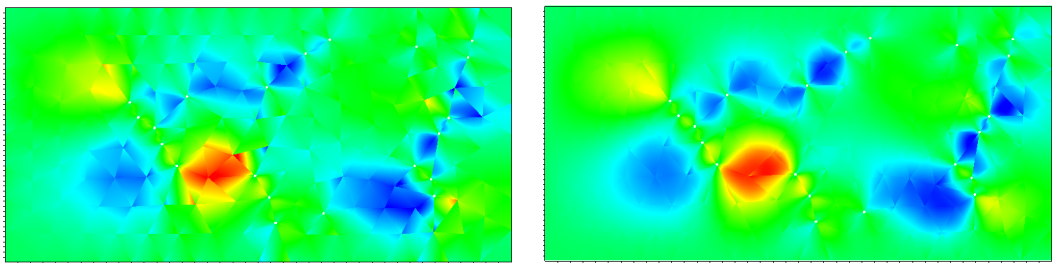

(a) CR2 8×16 (b) CR3 8×16

Figure 7: Comparison of u_y contours computed with CR2 and CR3 methods

where $\mathcal{E}_H(T_k)$ is the set of all the edges of the triangle T_k.

This equation is implemented using the FVEM in TrioCFD software with the P1NC-P0 finite element space. In the weak form, this equation reduces to finding $\boldsymbol{\Phi}_{E,i} \in H^1(T_k \cap \Omega^\epsilon)^d$, $\pi_{E,i} \in L^2_0(T_k \cap \Omega^\epsilon)$, and the Lagrange multipliers $\lambda_{F,j} \in \mathbb{R}$, $\forall F \in \mathcal{E}_H(T_k)$ and $j = 1, ..., s$ by solving:

$$\int_{T_k \cap \Omega^\epsilon} \nabla \boldsymbol{\Phi}_{E,i} : \nabla \boldsymbol{v} - \int_{T_k \cap \Omega^\epsilon} \pi_{E,i} \, \mathrm{div} \boldsymbol{v} + \sum_{F \in \mathcal{E}(T_k)} \lambda_{F,j} \cdot \int_F \boldsymbol{v} \cdot \boldsymbol{\omega_{F,j}} = 0, \tag{6}$$

$$\forall \boldsymbol{v} \in H^1(T_k) \text{ such that } \boldsymbol{v} = 0 \text{ on } T_k \cap B^\epsilon$$

$$\int_{T_k \cap \Omega^\epsilon} q \, \mathrm{div} \boldsymbol{\Phi}_{E,i} = 0, \ \forall q \in L^2_0(T_k \cap B^\epsilon)$$

$$\sum_{F \in \mathcal{E}(T_k)} \mu_{F,j} \cdot \int_F \boldsymbol{\Phi}_{E,i} \cdot \boldsymbol{\omega}_{F,j} = \mu_{E,i}, \ \forall \boldsymbol{\mu}_F \in \mathbb{R}^d, \ F \in \mathcal{E}(T_k)$$

3.4 Crouzeix-Raviart MsFEM coarse-scale solution

We now define the coarse-scale solution of Eq.(1). By discretising p into p_H and $\boldsymbol{u}$ into $\boldsymbol{u}_H$, we reformulate Eq.(1) in a weak form in τ_H as:

$$a(\boldsymbol{u}_H, \boldsymbol{v}_H) + b(\boldsymbol{v}_H, \bar{p}_H) = (\boldsymbol{v}_H, \boldsymbol{f}), \ \forall \boldsymbol{v}_H \in V_H \tag{7}$$

$$b(\boldsymbol{u}_H, q_H) = 0, \ \forall q_H \in M_H$$

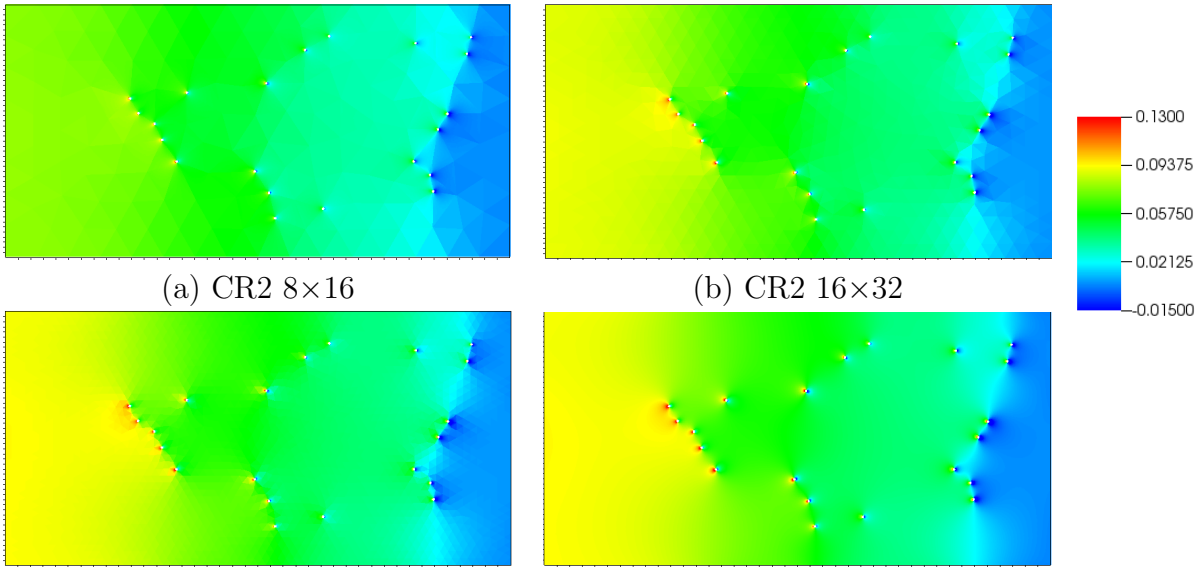

(a) CR2 8×16 (b) CR2 16×32

(a) CR2 32×64 (b) Reference

Figure 8: Pressure contours of a channel flow with CR2 method

where

$$a\left(\boldsymbol{u}_H, \boldsymbol{v}_H\right) = \int_{\Omega^\epsilon} \mu \nabla \boldsymbol{u}_H : \nabla \boldsymbol{v}_H \, \mathrm{dV} \tag{8}$$
$$b\left(\boldsymbol{v}_H, \bar{p}_H\right) = -\int_{\Omega^\epsilon} \bar{p}_H \nabla \cdot \boldsymbol{v}_H \, \mathrm{dV}$$

The solution of problem can then approximated as linear combination of multiscale basis functions $\boldsymbol{\Phi}_{E,i}$:

$$\boldsymbol{u}_H\left(x,y\right) = \sum_{E\in\mathcal{E}(T_k)} \sum_{i=1}^{s} u_{E,i} \boldsymbol{\Phi}_{E,i}\left(x,y\right) \tag{9}$$
$$p_H\left(x,y\right) = \sum_{E\in\mathcal{E}(T_k)} \sum_{i=1}^{s} u_{E,i} \pi_{E,i}\left(x,y\right) + \bar{p}_H$$

The coarse-scale problem is solved on the coarse mesh τ_H using P1NC-P0 finite element method implemented in TrioCFD. We calculate reference solutions using a P1NC-P0 finite element method in the global fine mesh τ_h. All systems are solved by the pressure-correction algorithm [9, 10] which is widely used in industrial softwares.

3.5 Choices of weighting functions

In this article, we consider two choices of weighting functions, leading to two different multiscale spaces [2]:

$$\begin{aligned} &\mathrm{CR2}: s=2,\ \boldsymbol{\omega}_{E,1}=\boldsymbol{e}_1,\ \boldsymbol{\omega}_{E,2}=\boldsymbol{e}_2. \\ &\mathrm{CR3}: s=3,\ \boldsymbol{\omega}_{E,1}=\boldsymbol{e}_1,\ \boldsymbol{\omega}_{E,2}=\boldsymbol{e}_2,\ \boldsymbol{\omega}_{E,3}=\boldsymbol{n}_E\Psi_E \end{aligned} \tag{10}$$

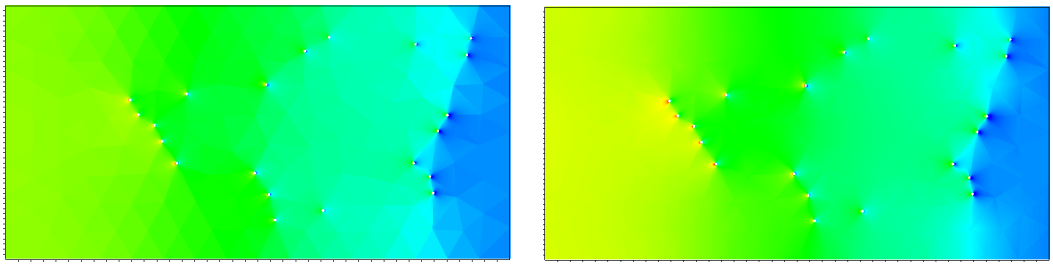

(a) CR2 8×16 (b) CR3 8×16

Figure 9: Comparison of pressure contours computed with CR2 and CR3 methods

for any $E \in \mathcal{E}_H$. Here $\boldsymbol{n}_E$ denote a unit vector normal to E and Ψ_E a linear polynomial on E such that $\int_E \Psi_E = 0$. $\boldsymbol{n}_E$ and Ψ_E are arbitrary, but should be made once for all.

4 NUMERICAL RESULTS

We consider a 2 dimensional channel $\Omega = [0 \leq x \leq 2, 0 \leq y \leq 1]$ containing a porous medium spanning from $x = 0$ to $x = 2$. We assign $\rho = 1$, $\mu = 1$, and $\boldsymbol{f} = 0$. At the inlet, the theoretical incompressible Poiseuille solution (parabolic velocity profile) is applied for all cases, i.e. $\boldsymbol{u} = 0.004y\,(1-y)\,\boldsymbol{e}_1$ on $x = 0$, whereas the Neumann boundary condition $\partial\boldsymbol{u}/\partial\boldsymbol{n} = 0$ is assumed at the outlet $x = 2$. No-slip boundary conditions are applied at the top and bottom walls.

First, we apply our method on a simple Poiseuille flow without any inclusions. Then we consider a open-channel flow in a heterogenous medium with 21 inclusions, each with a width of $\varepsilon = 0.01$ depicted in Fig. 3. The reference solution is calculated on a fine mesh of environ 320×640 triangles.

4.1 Poiseuille flow

For the Poiseuille flow, the error norms of the Crouzeix-Raviart MsFEM solutions relative to the theoretical solution on a number of coarse meshes are given in the left figure of Fig. 10, showing a convincingly converging trend.

4.2 Open-channel flow in a heterogenous medium

In the presence of random pattern of inclusions (see Fig 3), the Reynolds number is $Re = 0.001$ where $Re = \dfrac{\rho\varepsilon|\boldsymbol{u}|}{\mu}$ (in the absence of inclusions, ε is the channel diameter).

4.2.1 Numerical results with CR2 method

In Figs. 4 and 5, solutions of CR2 method on several mesh configurations in terms of u_x and u_y contours are given alongside those of the reference solutions. In Fig. 8,the pressure contours are given. From Fig. 10 we can see that our results converge toward the reference solutions. Most flow features can be quantitatively captured using the configuration 16×32.

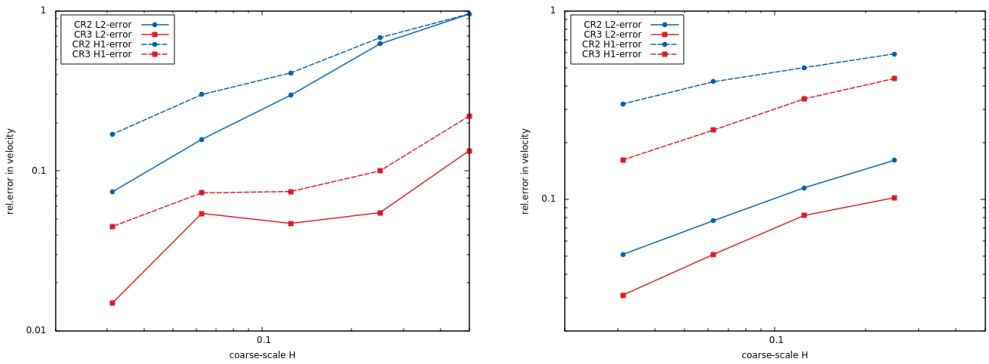

Figure 10: Left: relative errors of Poiseille flow. Right: relative errors of channel flow.

4.2.2 Comparison of numerical results with CR2 and CR3 methods

Authors of [7] point out that CR2 space V_H method may not be sufficient in some cases to construct a suitable approximation of the solution to the Stokes problem. Thus the CR3 method has been implemented in TrioCFD in order to enrich multi-scale basis functions and ameliorate the accuracy of our numerical results. From Figs. 6 and 7, we observe that the CR3 method captures better the flows features and shows less non-conformity than the CR2 method. In Fig. 9, we observe that the CR3 method gives slightly better pressure than the CR2 method. From Fig. 10, we can see that CR3 gives smaller L^2 and H^1 errors compared to the CR2 method.

5 CONCLUSIONS

In this paper, two variants (CR2 and CR3) of Crouzeix-Raviart MsFEM has been developed and implemented in TrioCFD. Numerical tests have been done for imcompressible flow around very fine and non-periodically placed inclusions. The Crouzeix-Raviart multiscale basis functions are computed in triangular discretisation by FVEM in TrioCFD and belong to P1NC-P0 FEM spaces. The weakly enforced continuity across coarse element edges ensures accurate basis function solutions without using any oversampling methods. Convergence studies of Poiseuille flow and open-channel flow in heterogeneous media are given. Good qualitative agreement with the reference solutions has been shown at relativement coarse mesh configurations.

However, CR2 may be insufficient to approximate accurately the solutions of Stokes flow. With the enrichment of basis functions, CR3 method captures better flow features and improves the accuracy of the MsFEM especially in presence of very dense inclusions. Other types of enrichment of basis functions can be a subject of our future work.

This work has layed the ground work for more complicated Navier-Stokes equations. Using basis functions computed by solving Stokes equations, our current work is developping different convection schemes to solve the Navier-Stokes coarse problem.

Although the test cases are given in 2 dimensions, the MsFEM have been developed and implemented in TrioCFD for 2 and 3 dimensions cases. More simulation results will be presented later.

6 ACKNOWLEDGEMENT

This work was done with granted access to the HPC resources of CINES under the allocation A0032A07571 made by GENCI. The authors thank Alexei Lozinski and Francis Kloss who have provided insight and expertise that greatly assisted the work.

REFERENCES

[1] Y Efendiev and T Y Hou. Multiscale Finite Element Methods, theory and applications. *Surveys and tutorials in the applied mathematical sciences, Springer*, 2:202, 2007.

[2] B P Muljadi, J Narski, A Lozinski, and P Degond. Non-conforming multiscale finite element method for Stokes flows in heterogeneous media. Part I: methodologies and numerical experiments. *SIAM Multiscale Modeling & Simulation*, 13(4):1146–1172, 2015.

[3] T. Y. Hou and X. H. Wu. A multiscale finite element method for elliptic problems in composite materials and porous media. *Journal of Computational Physics*, 134(1):169–189, 1997.

[4] M Crouzeix and P.-A. Raviart. Conforming and nonconforming finite element methods for solving the stationary Stokes equations I. *ESAIM: Mathematical Modelling and Numerical Analysis - Modélisation Mathématique et Analyse Numérique*, 7(3):33–75, 1973.

[5] Claude Le Bris, Frédéric Legoll, and Alexei Lozinski. MsFEM à la Crouzeix-Raviart for Highly Oscillatory Elliptic Problems. *Chinese Annals of Mathematics. Series B*, 34(1):113–138, 2013.

[6] Claude Le Bris, Frédéric Legoll, and Alexei Lozinski. An MsFEM Type Approach for Perforated Domains. *Multiscale Modeling & Simulation*, 12(3):1046–1077, 2014.

[7] G Jankowiak and A Lozinski. Non-Conforming Multiscale Finite Element Method for Stokes Flows in Heterogeneous Media. Part II: Error estimates for periodic microstructure. *ArXiv e-prints*, 13(4):1146–1172, 2018.

[8] CEA/DEN/DM2S/STMF/LMSF. http://www-trio-u.cea.fr.

[9] A.J. Chorin. Numerical solution of the Navier-Stokes equations. *Mathematics of Computation*, 22:745–762, 1968.

[10] J L Guermond and L Quartapelle. On the aproximation of the unsteady Navier-Stokes equations by finite element projection methods. *Numerische Mathematik*, 80(2):207–238, 1998.